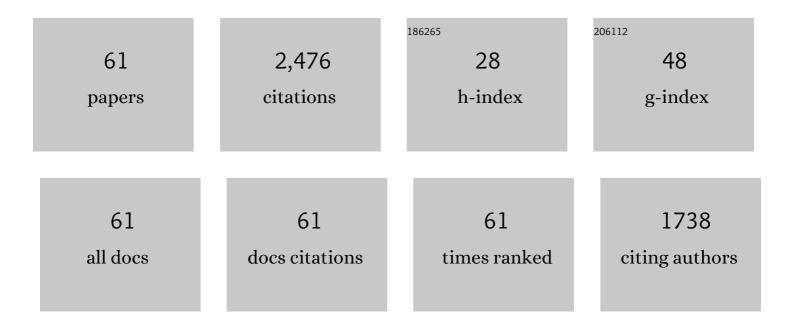
Yuebing Xu

List of Publications by Year in descending order

Source: https://exaly.com/author-pdf/3472256/publications.pdf Version: 2024-02-01



YHERING XII

#	Article	IF	CITATIONS
1	Insights into the Influence of CeO ₂ Crystal Facet on CO ₂ Hydrogenation to Methanol over Pd/CeO ₂ Catalysts. ACS Catalysis, 2020, 10, 11493-11509.	11.2	391
2	Hydrogenation of CO ₂ into hydrocarbons: enhanced catalytic activity over Fe-based Fischer–Tropsch catalysts. Catalysis Science and Technology, 2018, 8, 4097-4107.	4.1	123
3	Selective production of aromatics from CO ₂ . Catalysis Science and Technology, 2019, 9, 593-610.	4.1	120
4	Insights into the influence of support and potassium or sulfur promoter on iron-based Fischer–Tropsch synthesis: understanding the control of catalytic activity, selectivity to lower olefins, and catalyst deactivation. Catalysis Science and Technology, 2017, 7, 1245-1265.	4.1	98
5	Conversion of syngas toward aromatics over hybrid Fe-based Fischer-Tropsch catalysts and HZSM-5 zeolites. Applied Catalysis A: General, 2018, 552, 168-183.	4.3	82
6	Ironâ€Based Fischer–Tropsch Synthesis for the Efficient Conversion of Carbon Dioxide into Isoparaffins. ChemCatChem, 2016, 8, 1303-1307.	3.7	80
7	Unraveling Reactivity Descriptors and Structure Sensitivity in Low-Temperature NH ₃ -SCR Reaction over CeTiO <i>_x</i> Catalysts: A Combined Computational and Experimental Study. ACS Catalysis, 2021, 11, 7613-7636.	11.2	75
8	Particle size effects in the selective hydrogenation of cinnamaldehyde over supported palladium catalysts. RSC Advances, 2016, 6, 75541-75551.	3.6	66
9	Effect of transition metal additives on the catalytic stability of Mo/HZSM-5 in the methane dehydroaromatization under periodic CH4–H2 switch operation at 1073K. Applied Catalysis A: General, 2011, 409-410, 181-193.	4.3	62
10	A clue to exploration of the pathway of coke formation on Mo/HZSM-5 catalyst in the non-oxidative methane dehydroaromatization at 1073K. Applied Catalysis A: General, 2014, 482, 387-396.	4.3	62
11	The effect of zeolite particle size on the activity of Mo/HZSM-5 in non-oxidative methane dehydroaromatization. Applied Catalysis A: General, 2011, 393, 348-358.	4.3	61
12	The distribution of coke formed over a multilayer Mo/HZSM-5 fixed bed in H2 co-fed methane aromatization at 1073 K: Exploration of the coking pathway. Journal of Catalysis, 2015, 330, 261-272.	6.2	61
13	The catalytic stability of Mo/HZSM-5 in methane dehydroaromatization at severe and periodic CH4–H2 switch operating conditions. Chemical Engineering Journal, 2011, 168, 390-402.	12.7	60
14	Insight into the Intrinsic Active Site for Selective Production of Light Olefins in Cobalt-Catalyzed Fischer–Tropsch Synthesis. ACS Catalysis, 2019, 9, 7073-7089.	11.2	60
15	Investigation of the highly tunable selectivity to linear α-olefins in Fischer–Tropsch synthesis over silica-supported Co and CoMn catalysts by carburization–reduction pretreatment. Catalysis Science and Technology, 2017, 7, 4736-4755.	4.1	53
16	Sodium-Mediated Bimetallic Fe–Ni Catalyst Boosts Stable and Selective Production of Light Aromatics over HZSM-5 Zeolite. ACS Catalysis, 2021, 11, 3553-3574.	11.2	50
17	Improving effect of Fe additive on the catalytic stability of Mo/HZSM-5 in the methane dehydroaromatization. Catalysis Today, 2012, 185, 41-46.	4.4	46
18	Particle-Size-Dependent Methane Selectivity Evolution in Cobalt-Based Fischer–Tropsch Synthesis. ACS Catalysis, 2020, 10, 2799-2816.	11.2	46

YUEBING XU

#	Article	IF	CITATIONS
19	Coke accumulation and deactivation behavior of microzeolite-based Mo/HZSM-5 in the non-oxidative methane aromatization under cyclic CH 4 -H 2 feed switch mode. Applied Catalysis A: General, 2017, 530, 12-20.	4.3	45
20	CO ₂ formation mechanism in Fischer–Tropsch synthesis over iron-based catalysts: a combined experimental and theoretical study. Catalysis Science and Technology, 2018, 8, 5288-5301.	4.1	45
21	Probing cobalt localization on HZSM-5 for efficient methane dehydroaromatization catalysts. Journal of Catalysis, 2020, 387, 102-118.	6.2	43
22	Direct production of aromatics from syngas over a hybrid FeMn Fischer–Tropsch catalyst and HZSM-5 zeolite: local environment effect and mechanism-directed tuning of the aromatic selectivity. Catalysis Science and Technology, 2019, 9, 3933-3946.	4.1	41
23	Supported Fe/MnO _x catalyst with Ag doping for remarkably enhanced catalytic activity in Fischer–Tropsch synthesis. Catalysis Science and Technology, 2018, 8, 1953-1970.	4.1	38
24	Comparison of the activity stabilities of nanosized and microsized zeolites based Fe–Mo/HZSM-5 catalysts in the non-oxidative CH4 dehydroaromatization under periodic CH4–H2 switching operation at 1073K. Applied Catalysis A: General, 2013, 452, 105-116.	4.3	35
25	Dependence of copper particle size and interface on methanol and CO formation in CO ₂ hydrogenation over Cu@ZnO catalysts. Catalysis Science and Technology, 2022, 12, 551-564.	4.1	33
26	Assessing the formation of cobalt carbide and its catalytic performance under realistic reaction conditions and tuning product selectivity in a cobalt-based FTS reaction. Catalysis Science and Technology, 2019, 9, 3238-3258.	4.1	32
27	Experimental Investigation on the Two-Sided Effect of Acidic HZSM-5 on the Catalytic Performance of Composite Fe-Based Fischer–Tropsch Catalysts and HZSM-5 Zeolite in the Production of Aromatics from CO ₂ /H ₂ . Industrial & Engineering Chemistry Research, 2020, 59, 8581-8591.	3.7	31
28	Selective mild oxidation of methane to methanol or formic acid on Fe–MOR catalysts. Catalysis Science and Technology, 2019, 9, 6946-6956.	4.1	29
29	Suppressing C–C Bond Dissociation for Efficient Ethane Dehydrogenation over the Isolated Co(II) Sites in SAPO-34. ACS Catalysis, 2021, 11, 13001-13019.	11.2	29
30	CH ₄ conversion over Ni/HZSM-5 catalyst in the absence of oxygen: decomposition or dehydroaromatization?. Chemical Communications, 2020, 56, 4396-4399.	4.1	28
31	Experimental evidence for three rate-controlling regions of the non-oxidative methane dehydroaromatization over Mo/HZSM-5 catalyst at 1073 K. Catalysis Science and Technology, 2011, 1, 823.	4.1	26
32	Identification of atomically dispersed Fe-oxo species as new active sites in HZSM-5 for efficient non-oxidative methane dehydroaromatization. Journal of Catalysis, 2021, 396, 224-241.	6.2	25
33	Effect of superficial velocity on the coking behavior of a nanozeolite-based Mo/HZSM-5 catalyst in the non-oxidative CH4 dehydroaromatization at 1073 K. Catalysis Science and Technology, 2013, 3, 2769.	4.1	24
34	Catalytic cracking of coal-tar model compounds over ZrO2/Al2O3 and Ni-Ce/Al2O3 catalysts under steam atmosphere. Fuel, 2020, 263, 116763.	6.4	24
35	Comparison of the activities of binder-added and binder-free Mo/HZSM-5 catalysts in methane dehydroaromatization at 1073 K in periodic CH4-H2 switch operation mode. Journal of Natural Gas Chemistry, 2012, 21, 729-744.	1.8	23
36	Performance of a binder-free, spherical-shaped Mo/HZSM-5 catalyst in the non-oxidative CH4 dehydroaromatization in fixed- and fluidized-bed reactors under periodic CH4–H2 switch operation. Chemical Engineering and Processing: Process Intensification, 2013, 72, 90-102.	3.6	21

YUEBING XU

#	Article	IF	CITATIONS
37	Investigation on converting 1-butene and ethylene into propene <i>via</i> metathesis reaction over W-based catalysts. RSC Advances, 2018, 8, 8372-8384.	3.6	21
38	Investigation of the deactivation behavior of Co catalysts in Fischer–Tropsch synthesis using encapsulated Co nanoparticles with controlled SiO2 shell layer thickness. Catalysis Science and Technology, 2020, 10, 1182-1192.	4.1	21
39	Insight into the active site and reaction mechanism for selective oxidation of methane to methanol using H ₂ O ₂ on a Rh ₁ /ZrO ₂ catalyst. New Journal of Chemistry, 2020, 44, 1632-1639.	2.8	20
40	Identifying the crucial role of water and chloride for efficient mild oxidation of methane to methanol over a [Cu2(μ-O)]2+-ZSM-5 catalyst. Journal of Catalysis, 2022, 405, 1-14.	6.2	19
41	MCM-41 supported CuO/Bi2O3 nanoparticles as potential catalyst for 1,4-butynediol synthesis. Ceramics International, 2014, 40, 3969-3973.	4.8	17
42	A Facile Fabrication of Supported Ni/SiO2 Catalysts for Dry Reforming of Methane with Remarkably Enhanced Catalytic Performance. Catalysts, 2019, 9, 183.	3.5	17
43	Dehydrogenation of n-butane over vanadia catalysts supported on silica gel. Journal of Natural Gas Chemistry, 2009, 18, 88-93.	1.8	16
44	A binder-free fluidizable Mo/HZSM-5 catalyst for non-oxidative methane dehydroaromatization in a dual circulating fluidized bed reactor system. Catalysis Today, 2017, 279, 115-123.	4.4	16
45	Fischer-Tropsch synthesis to lower α-olefins over cobalt-based catalysts: Dependence of the promotional effect of promoter on supports. Catalysis Today, 2021, 369, 158-166.	4.4	16
46	Experimental investigation of the promotion effect of CO on catalytic behavior of Mo/HZSM-5 catalyst in CH4 dehydroaromatization at 1073ÂK. Fuel, 2020, 262, 116674.	6.4	15
47	A rapid and effective method for evaluating the initial activity of Mo/HZSM-5 catalyst in the methane dehydroaromatization reaction at severe conditions. Catalysis Communications, 2010, 12, 127-131.	3.3	14
48	Distinguishing external and internal coke depositions on micron-sized HZSM-5 <i>via</i> catalyst-assisted temperature-programmed oxidation. New Journal of Chemistry, 2019, 43, 13938-13946.	2.8	14
49	Mechanism of Fe additive improving the activity stability of microzeolite-based Mo/HZSM-5 catalyst in non-oxidative methane dehydroaromatization at 1073 K under periodic CH ₄ –H ₂ switching modes. Catalysis Science and Technology, 2014, 4, 3644-3656.	4.1	13
50	NGU: Development of a twoâ€bed circulating fluidized bed reactor system for nonoxidative aromatization of methane over Mo/HZSMâ€5 catalyst. Environmental Progress and Sustainable Energy, 2016, 35, 325-333.	2.3	13
51	Catalytic Activity for CO ₂ Hydrogenation is Linearly Dependent on Generated Oxygen Vacancies over CeO ₂ ‣upported Pd Catalysts. ChemCatChem, 2022, 14, .	3.7	13
52	Insight into the anti-coking ability of NiM/SiO2 (M=ZrO2, Ru) catalyst for dry reforming of CH4 to syngas. International Journal of Hydrogen Energy, 2022, 47, 2268-2278.	7.1	12
53	Tuning the Lewis acidity of ZrO ₂ for efficient conversion of CH ₄ and CO ₂ into acetic acid. New Journal of Chemistry, 2021, 45, 8978-8985.	2.8	9
54	Effect of Bed Height on the Performance of a Fixed Mo/HZSMâ€5 Bed in Direct Aromatization of Methane. Chemical Engineering and Technology, 2016, 39, 2059-2065.	1.5	8

YUEBING XU

#	Article	IF	CITATIONS
55	Unravelling the structure-performance relationship over iron-based Fischer-Tropsch synthesis by depositing the iron carbonyl in syngas on SiO2 in a fixed-bed reactor. Applied Catalysis A: General, 2019, 572, 197-209.	4.3	8
56	Effect of kaolinites modified with Zr and transition metals on the pyrolysis behaviors of low-rank coal and its model compound. Journal of the Energy Institute, 2021, 95, 41-51.	5.3	7
57	Pore-Confined and Diffusion-Dependent Olefin Catalytic Cracking for the Production of Propylene over SAPO Zeolites. Industrial & Engineering Chemistry Research, 2022, 61, 7760-7776.	3.7	7
58	Stable co-production of olefins and aromatics from ethane over Co ²⁺ -exchanged HZSM-5 zeolite. Catalysis Science and Technology, 2022, 12, 3716-3726.	4.1	4
59	Insights into Fe Species Structureâ€Performance Relationship for Direct Methane Conversion toward Oxygenates over Feâ€MOR Catalysts. ChemCatChem, 2022, 14, .	3.7	4
60	Structural evolution of large Fe ₃ O ₄ microspheres on graphene oxide for efficient conversion of syngas into α-olefins. New Journal of Chemistry, 2020, 44, 4987-4991.	2.8	2
61	Development of catalysts for direct non-oxidative methane aromatization. , 2022, 1, 80-92.		2